Co-prime Sampling based Gridless Time-Delay Estimation for Ground Penetrating Radar System with Enhanced Single Measurement Vector

Huimin Pan, Jingjing Pan, Xiaofei Zhang, Yide Wang

Co-prime Sampling based Gridless Time-Delay Estimation for Ground Penetrating Radar System with Enhanced Single Measurement Vector

Huimin Pan, Jingjing Pan, *Member, IEEE*, Xiaofei Zhang, and Yide Wang, *Senior Member, IEEE*

***Abstract*—Time-delay estimation (TDE) holds great significance in pavement surveys, especially in the modern transportation system. Established on the ideal Dirac pulse and white Gaussian noise, the performance of the existing TDE methods may degrade in practical ground penetrating radar (GPR) detection, where radar pulse and noise distribution are diverse. In this letter, we develop a gridless TDE method considering the radar pulse and noise pattern in GPR detection. Co-prime sampling strategy is applied to reduce the number of frequency samples compared with conventional uniform sampling. With the prior knowledge of radar pulse and noise distribution, an enhanced measurement vector is generated from the data covariance matrix, thus improves the signal quality compared with the conventional methods simply assuming ideal Dirac pulse and white Gaussian noise. Subsequently, the time-delays are estimated by the proposed atomic norm minimization (ANM) method, where the complexity is further reduced compared with the previous works using multiple measurements. Simulation results show the advantages of the proposed method in terms of running time, weak echo detection, and estimation accuracy.**

***Index Terms*—Time-delay estimation (TDE), ground penetrating radar (GPR), coherent signals, radar pulse, noise pattern, atomic norm minimization (ANM).**

I. Introduction

In transportation system, ground penetrating radar (GPR) [1] is a non-destructive tool for pavement quality assessment and road maintenance. From the GPR profile, the structure of stratified pavement can be described by means of time-delay estimation (TDE) and amplitude estimation. Especially, TDE provides the thickness of each layer. Significant research has been done to estimate the time-delays of GPR echoes over the last few decade [2], [3].

One of the main obstacles for TDE is the dense sampling points due to the uniform sampling strategy in GPR system with ultra wide bandwidth (UWB). To reduce the hardware burden, researchers have developed sparse sampling strategies [4]–[6], among which the co-prime strategy has been widely used thanks to its efficiency in system design. From the covariance matrix of co-prime sampled signals, the virtual sampling is constructed with limited physical samplers in a virtual manner. However, it is not applicable to TDE owing to the inner coherency between the GPR echoes. Moreover, the "holes" in co-prime sampling also prevent the high-resolution methods from the decoherence preprocessing techniques [7].

Compressive sensing (CS) [8], [9] provides a solution to exploit the sparse sampling strategy in the presence of coherent signals. The conventional CS methods, e.g., sparse Bayesian interference (SBI) [8] and orthogonal matching pursuit (OMP) [9], [10], always perform poorly because of basis mismatch when the targets are off-grid. To this end, gridless methods are proposed to reconstruct the signals in a continuous atom set, among which atomic norm minimization (ANM) attracts attention from researchers. ANM [11]–[14] aims to recover the virtual covariance matrix, ignoring the "holes" and coherency among echoes. In [12], the single measurement vector (SMV) based ANM method has been successfully applied in line spectrum estimation. Then in [13], the multiple measurement vector (MMV) is proposed to enhance the reconstruction accuracy, requiring a heavier complexity to solve the large semi-definite programming (SDP) in ANM problem. Later, our previous work [14] develops the MMV-ANM method for TDE in GPR system, where the number of variables are reduced in the two-level SDP problem.

Another difficulty comes from the radar pulse and noise pattern in practical GPR system. In the previous work, the radar pulse is assumed to be an ideal Dirac pulse. But in the impulse or step-frequency system, the GPR pulse is not flat over the selected bandwidth because of the antenna response [1], [2], [15]. Although data whitening preprocessing [1] can be applied to remove the non-linear exponential behaviour of radar pulse, the noise pattern is changed, leading to a non-Gaussian-white noise and the data model mismatch.

Driven by these observations, in this letter, we propose a co-prime sampling based gridless TDE method for GPR system considering the radar pulse and noise pattern. The contributions of this letter are summarized as follows: 1) we generate an enhanced SMV from the eigen-space of data covariance matrix, taking into account the radar pulse and noise pattern; 2) the enhanced SMV also promotes the detection and estimation performance of weak echoes compared with those methods simply considering ideal scenarios; 3) the complexity of proposed method is greatly reduced with a smaller SDP scale compared with that in MMV-ANM [14].

II. Data Model

Usually, the studied pavement is assumed to be horizontally stratified, and the media are homogeneous and low-loss [1]–[3]. Consider an pavement with K interfaces, the received

H. Pan, J. Pan, and X. Zhang are with College of Electronic and Information Engineering, Nanjing University of Aeronautics and Astronautics, 211106 Nanjing, China.

Y. Wang is with the Institut d'Electronique et des Technologies du NumeRique (IETR), CNRS UMR6164, Nantes University, 44306 Nantes, France.

Manuscript received 2024.

signal by a GPR is then composed of K coherent echoes with corresponding time shift and attenuation. The received signal is modeled in frequency domain as [1]

$$r(f) = \sum_{k=1}^{K} s_0 \alpha_k \tilde{e}(f) e^{-j2\pi f \tau_k} + n(f), \tag{1}$$

where s_0 is the emitted signal amplitude; α_k and τ_k denote the attenuation and arrival time corresponding to the kth echo, respectively; $\tilde{e}(f)$ is the frequency response of the radar pulse; $n(f)$ denotes the additive noise with zero mean. In the application of GPR detection, radar pulse $\tilde{e}(f)$ can be measured by backscattered echo from a metallic plane and thus is known beforehand as a prior knowledge in TDE problem.

In this letter, the received signal in (1) is sampled in frequency domain using co-prime sampling strategy. As shown in Fig. 1a, signals are sampled within $f \in [f_{\min}, f_{\max}]$, and the sampling points can be indicated by the following integer set

$$\begin{aligned} \mathbb{S} = & \left\{ l_i \middle| i = 1, 2, \cdots, M \right\} \\ = & \left\{ M_1 m \middle| m = 0, 1, \cdots, (f_{\max} - f_{\min})/(M_1 \Delta f) \right\} \\ & \cup \left\{ M_2 m \middle| m = 0, 1, \cdots, (f_{\max} - f_{\min})/(M_2 \Delta f) \right\}, \end{aligned} \tag{2}$$

where (M_1, M_2) is a pair of co-prime integers and M indicates the cardinality of set $\mathbb{S}$. Correspondingly, the sampling points in frequency domain are given by $f_i = f_{\min} + l_i \Delta f, l_i \in \mathbb{S}$, with the beginning frequency $f_1 = f_{\min}$ and the smallest interval Δf. Therefore, the co-prime sampling signal is modelled as

$$\mathbf{r} = s_0 \mathbf{\Lambda A} \boldsymbol{\alpha} + \mathbf{n} \tag{3}$$

with the following notations:

- $\mathbf{r} = [r(f_1), r(f_2), \cdots, r(f_M)]^T \in \mathbb{C}^{M \times 1}$ is the received signal vector, superscript $\{\cdot\}^T$ is the transpose operator;
- $\mathbf{\Lambda} = \text{diag}\{\tilde{e}(f_1), \tilde{e}(f_2), \cdots, \tilde{e}(f_M)\} \in \mathbb{C}^{M \times M}$ is a diagonal matrix whose entries are the frequency response of the radar pulse;
- $\mathbf{A} = [\mathbf{a}(\tau_1), \mathbf{a}(\tau_2), \cdots, \mathbf{a}(\tau_K)] \in \mathbb{C}^{M \times K}$ is the mode matrix, where the kth column $\mathbf{a}(\tau_k) = e^{-j2\pi f_1 \tau_k} [1, e^{-j2\pi l_2 \Delta f \tau_k}, \cdots, e^{-j2\pi l_M \Delta f \tau_k}]^T, l_i \in \mathbb{S}$ is defined as the mode vector of the kth echo; $\tau_k (k = 1, 2, \cdots, K)$ denotes the true arrival time of the kth echo;
- $\boldsymbol{\alpha} = [\alpha_1, \alpha_2, \cdots, \alpha_K]^T$ is the $K \times 1$ amplitude vector composed of attenuations of echoes; s_0 denotes the amplitude of the emitted signal;
- $\mathbf{n} = [n(f_1), n(f_2), \cdots, n(f_M)]^T \in \mathbb{C}^{M \times 1}$ is the noise vector with zero mean and colored Gaussian distribution.

To remove the non-linear exponential behaviour caused by radar pulse, the received signal is whiten as follows

$$\mathbf{x} = \mathbf{\Lambda}^{-1} \mathbf{r} = s_0 \mathbf{A} \boldsymbol{\alpha} + \mathbf{n}_w, \tag{4}$$

where $\mathbf{n}_w = \mathbf{\Lambda}^{-1} \mathbf{n}$ is the noise vector after data whitening. Since the noise is assumed to be statistically independent of the signal, the data covariance matrix of $\mathbf{x}$ can be expressed as

$$\mathbf{R} = \mathbb{E}\{\mathbf{x}\mathbf{x}^H\} = \mathbf{A}\mathbf{P}\mathbf{A}^H + \mathbf{\Sigma}, \tag{5}$$

where $\{\cdot\}^H$ is the conjugate transpose operator; $\mathbf{P} = \mathbb{E}\{(s_0 \boldsymbol{\alpha})(s_0 \boldsymbol{\alpha})^H\} = s_0^2 \boldsymbol{\alpha}\boldsymbol{\alpha}^H$ is the source covariance matrix and $\mathbf{\Sigma} = \mathbb{E}\{\mathbf{n}_w \mathbf{n}_w^H\}$ is the covariance matrix of the colored noise $\mathbf{n}_w$. In addition, conventional decorrelation methods such as spatial smoothing preprocessing (SSP) [7] are impossible for restoring the rank of $\mathbf{P}$, because matrix $\mathbf{A}$ hasn't a Vandermonde structure due to the "holes".

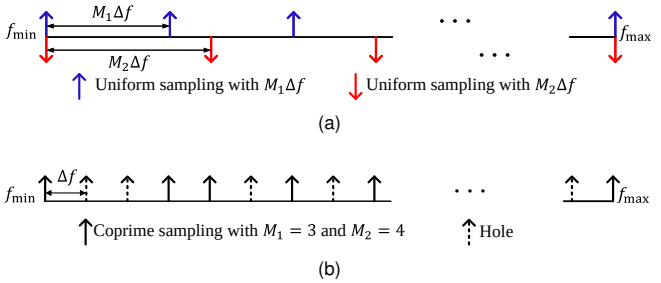

Fig. 1. Co-prime sampling strategy in frequency domain. (a) Sparse uniform samplings with $M_1\Delta f$ and with $M_2\Delta f$. (b) Co-prime sampling and the "holes" in the virtual uniform sampling.

III. Methodology

A. Generalized Eigenvalue Decomposition

In the previous literature, the TDE methods assume the ideal Dirac radar pulse and additive white Gaussian noise. However, in practical GPR system, the influence from noise pattern $\mathbf{\Sigma}$ is not negligible. Hence, the proposed method exploits the characteristics of radar pulse and noise pattern to enhance the signal. The GEVD between $\mathbf{R}$ and $\mathbf{\Sigma}$ is defined as [16]

$$\mathbf{R}\mathbf{u}_m = \lambda_m \mathbf{\Sigma}\mathbf{u}_m, m = 1, 2, \cdots, M, \tag{6}$$

where λ_m is the mth eigenvalue, and $\mathbf{u}_m \in \mathbb{C}^{M \times 1}$ is the corresponding eigenvector. Since the echoes are coherent, only the largest generalized eigenvalue λ_1 and its corresponding generalized eigenvector $\mathbf{u}_1$ are associated to the echoes. Particularly, $\mathbf{u}_1$ is proved to be the optimal projector, which maximizes the projected signal-to-noise ratio (SNR) [16] defined as $\frac{P_s(\mathbf{u})}{P_n(\mathbf{u})} = \frac{\mathbf{u}^H \mathbf{A}\mathbf{P}\mathbf{A}^H \mathbf{u}}{\mathbf{u}^H \mathbf{\Sigma} \mathbf{u}}$. Then, subtract $\mathbf{\Sigma}\mathbf{u}_1$ from both sides of $\mathbf{R}\mathbf{u}_1 = \lambda_1 \mathbf{\Sigma}\mathbf{u}_1$, we have

$$\mathbf{A}\mathbf{P}\mathbf{A}^H \mathbf{u}_1 = (\lambda_1 - 1)\mathbf{\Sigma}\mathbf{u}_1. \tag{7}$$

Let $\mathbf{g} = \mathbf{P}\mathbf{A}^H \mathbf{u}_1$, an enhanced single measurement vector $\mathbf{x}_{\mathbb{S}}$ can be formulated as

$$\mathbf{x}_{\mathbb{S}} = \mathbf{A}\mathbf{g} = (\lambda_1 - 1)\mathbf{\Sigma}\mathbf{u}_1, \tag{8}$$

which is a linear combination of the columns of $\mathbf{A}$. In this way, the influence of radar pulses and noise distribution is taken into account to obtain a matched, exact, therefore enhanced signal model. It is worth mentioning that the classical methods are often based on the hypotheses of the ideal Dirac pulse and white Gaussian noise, resulting in a mismatched data model.

B. Atomic Norm Minimization

Imagine that a virtual uniform sampling is obtained, shown as Fig.1b, the sampling points are positioned by the integer set $\mathbb{V}$ with successive integer elements

$$\mathbb{V} = \{l, 0 \le l \le L - 1\}, \tag{9}$$

whose cardinality is $L = \max\{\mathbb{S}\}$. In the GPR system using co-prime sampling strategy, the received signal is the partial observation of the virtual uniform sampling, given by

$$[\hat{\mathbf{x}}_{\mathbb{V}}]_{l_i} = \begin{cases} [\mathbf{x}_{\mathbb{S}}]_i, & l_i \in \mathbb{S} \\ 0, & l_i \notin \mathbb{S} \end{cases}, l_i = 1, 2, \cdots, L\,, \tag{10}$$

where $[\hat{\mathbf{x}}_{\mathbb{V}}]_{l_i}$ denotes the l_ith element of $\hat{\mathbf{x}}_{\mathbb{V}}$ while $[\mathbf{x}_{\mathbb{S}}]_l$ represents the lth element of $\mathbf{x}_{\mathbb{S}}$.

By filling the "holes" in (10), the corresponding single measurement using uniform sampling is recovered as

$$\mathbf{x}_{\mathbb{V}} = \mathbf{A}_{\mathbb{V}}\mathbf{g}, \tag{11}$$

where $\mathbf{A}_{\mathbb{V}} = [\mathbf{a}_{\mathbb{V}}(\tau_1), \mathbf{a}_{\mathbb{V}}(\tau_2), \cdots, \mathbf{a}_{\mathbb{V}}(\tau_K)] \in \mathbb{C}^{L\times K}$ is the mode matrix of uniform sampling whose columns are defined as $\mathbf{a}_{\mathbb{V}}(\tau_k) = [1, e^{-j2\pi\Delta f\tau_k}, \cdots, e^{-j2\pi(L-1)\Delta f\tau_k}]^T \in \mathbb{C}^{L\times 1}, k = 1, 2, \cdots, K$. The source vector is denoted by $\mathbf{g} = [g_1, g_2, \cdots, g_K]^T$, and $g_k = e^{-j\psi_k}\rho_k$ is its kth entry with phase ψ_k and amplitude $\rho_k > 0$. Define a diagonal matrix $\mathbf{\Gamma} = \text{diag}\{\rho_1, \rho_2, \cdots, \rho_K\} \in \mathbb{R}^{K\times K}$ and a phase vector $\boldsymbol{\psi} = [e^{-j\psi_1}, e^{-j\psi_2}, \cdots, e^{-j\psi_K}]^T$, $\mathbf{x}_{\mathbb{V}}$ can be decomposed as

$$\mathbf{x}_{\mathbb{V}} = \mathbf{A}_{\mathbb{V}}\mathbf{\Gamma}\boldsymbol{\psi}. \tag{12}$$

Define a selection vector $\mathbf{q} \in \mathbb{C}^L$ with the lth ($\forall l \in \mathbb{S}$) position being 1 and the other elements being 0, we have the relationship between observations (10) and (11) as

$$\hat{\mathbf{x}}_{\mathbb{V}} = \mathbf{x}_{\mathbb{V}} \odot \mathbf{q}, \tag{13}$$

where $\odot$ denotes the Hadamard product.

According to the idea of atomic norm in [12], $\mathbf{x}_{\mathbb{V}}$ can be described by a continuous-valued atom set

$$\mathcal{A} = \left\{ e^{-j\psi}\mathbf{a}_{\mathbb{V}}(\tau) \middle| \tau \in [t_{\min}, t_{\max}], \psi \in [-\pi, \pi] \right\}, \tag{14}$$

where $t_{\min}$ and $t_{\max}$ denote the beginning and end of time-delay searching range, respectively; ψ carries the phase offset of the atom. Then, the ℓ_0 atomic norm of $\mathbf{x}_{\mathbb{V}}$ is defined as

$$\|\mathbf{x}_{\mathbb{V}}\|_{\mathcal{A},0} = \inf_{K} \left\{ \mathbf{x}_{\mathbb{V}} = \sum_{k=1}^{K} \rho_k e^{-j\psi_k}\mathbf{a}_{\mathbb{V}}(\tau_k), \rho_k \geq 0 \right\}. \tag{15}$$

However, solving (15) is non-convex and NP-hard. A convex relaxation of $\|\mathbf{x}_{\mathbb{V}}\|_{\mathcal{A},0}$ is taken into consideration

$$\begin{aligned} \|\mathbf{x}_{\mathbb{V}}\|_{\mathcal{A}} &= \inf\{t > 0 : \mathbf{x}_{\mathbb{V}} \in t\ \text{conv}\{\mathcal{A}\}\} \\ &= \inf\left\{ \sum_{k=1}^{K} \rho_k \middle| \mathbf{x}_{\mathbb{V}} = \textstyle\sum_{k=1}^{K} \rho_k e^{-j\psi_k}\mathbf{a}_{\mathbb{V}}(\tau_k), \rho_k \geq 0 \right\} \end{aligned} \tag{16}$$

with $\text{conv}\{\mathcal{A}\}$ representing the convex hull of atom set $\mathcal{A}$. Furthermore, we can equivalently express the atomic norm of $\mathbf{x}_{\mathbb{V}}$ through the following theorem.

Theorem 1. *The atomic norm $\|\mathbf{x}_{\mathbb{V}}\|_{\mathcal{A}}$ is equivalent in a SDP form as:*

$$\begin{aligned} \|\mathbf{x}_{\mathbb{V}}\|_{\mathcal{A}} = \quad & \inf_{\mathcal{T}(\mathbf{z}),w} \left\{ \tfrac{1}{2L} tr(\mathcal{T}(\mathbf{z}) + \tfrac{1}{2}w \right\}, \\ \textit{subject to} \quad & \begin{bmatrix} \mathcal{T}(\mathbf{z}) & \mathbf{x}_{\mathbb{V}} \\ \mathbf{x}_{\mathbb{V}}^H & w \end{bmatrix} \succeq \mathbf{0}, \end{aligned} \tag{17}$$

where $\mathcal{T}(\mathbf{z}) = \mathbf{A}_{\mathbb{V}}\mathbf{\Gamma}\mathbf{A}_{\mathbb{V}}^H$ is a $L \times L$ Hermitian Toeplitz matrix with its first column $\mathbf{z} \in \mathbb{C}^{L\times 1}$; $w \geq \boldsymbol{\psi}^H\mathbf{\Gamma}\boldsymbol{\psi} = \sum_{k=1}^{K}\rho_k$ is a positive real value.

The proof of Theorem 1 is similar with the appendix in [14], except that the Hermitian matrix $\mathbf{W}$ is replaced by a real-valued variable w.

Considering the mismatch between the theoretical measurement $\mathbf{x}_{\mathbb{V}}$ and the observed signal $\hat{\mathbf{x}}_{\mathbb{V}}$, the atomic norm minimization problem to recover $\mathbf{x}_{\mathbb{V}}$ and $\mathcal{T}(\mathbf{z})$ is formulated as

$$\begin{aligned} \arg\min_{\mathcal{T}(\mathbf{z}),w} \quad & \mu\left\{\tfrac{1}{2L}\text{Tr}(\mathcal{T}(\mathbf{z})) + \tfrac{1}{2}w\right\} + \tfrac{1}{2}\|(\mathbf{x}_{\mathbb{V}} - \hat{\mathbf{x}}_{\mathbb{V}}) \odot \mathbf{q}\|_2^2, \\ \text{subject to} \quad & \begin{bmatrix} \mathcal{T}(\mathbf{z}) & \mathbf{x}_{\mathbb{V}} \\ \mathbf{x}_{\mathbb{V}}^H & w \end{bmatrix} \succeq \mathbf{0}, \end{aligned} \tag{18}$$

where μ is a positive regularization to balance the atomic norm and the fitting error term. Apparently, solution $\mathcal{T}(\mathbf{z})$ of (18) can be interpreted as the covariance matrix of $\mathbf{x}_{\mathbb{V}}$, removing the correlation between echoes. After applying MUSIC or root-MUSIC on $\mathcal{T}(\mathbf{z})$, the time-delays of GPR signals can be estimated.

IV. Performance Analysis

A. Complexity Analysis

Computational complexity is commonly used to evaluate the real-time processing performance of algorithms. According to [11], the scale of SDP contributes to the major computational complexity to solve convex optimization problems. In [14], the MMV-ANM is to recover two Toeplitz Hermitian matrices, indicating a complexity of $O((L+M)^{2.5}(M+1)^2(L+M/2)^{2.5})$. For ANM with a single measurement, the complexity is dramatically reduced to $O((L+1)^{2.5}(2L+1)^2)$. The proposed method required extra $O(M^3)$ to complete GEVD but the SDP scale is greatly reduced compared with that in MMV-ANM. The convergence speed of OGSBI relies on the iteration times N_{iter} and the number of grids n_g, resulting in computational cost $O(N_{\text{iter}}(M^3 + 2M^2n_g + 2M^2 + n_g^2M))$. Also, the complexity of the off-grid OMP (OGOMP) [9] method is given as $O(K(n_gJM + 2M))$ with J snapshots.

TABLE I provides the complexities of the proposed method, MMV-ANM [14], SMV-ANM [12], OMP [10], OGOMP [9] and OGSBI [8]. Fig. 2 compares the computational complexity of different algorithms, where the proposed algorithm needs far lower complexity than MMV-ANM and OGSBI.

TABLE I
THE MAXIMAL COMPLEXITY OF THE ALGORITHMS

Method	Complex number multiplication times
SMV-ANM [12]	$O(M^2J + L^3 + (L+1)^{2.5}(2L+1)^2)$
MMV-ANM [14]	$O(M^2J + L^3 + (L+M)^{2.5}(M+1)^2(L+M/2)^{2.5})$
OGSBI [8]	$O(N_{\text{iter}}(M^3 + 2M^2n_g + 2M^2 + n_g^2M))$
OMP [10]	$O(K(2Mn_g + 2M^3 + 4M))$
OGOMP [9]	$O(K(2Mn_g + 4M^3 + 4M))$
Proposed	$O(M^2J + M^3 + L^3 + (L+1)^{2.5}(2L+1)^2)$

B. Cramér-Rao Bound

The Cramér-Rao Bound (CRB) is a widely-used standard for assessing the performance of any unbiased estimator. Specifically, taking into account the radar pulse and noise

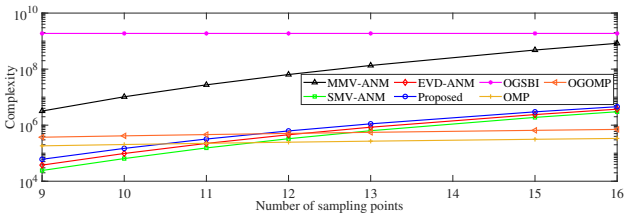

Fig. 2. Comparison of the maximal computational complexity.

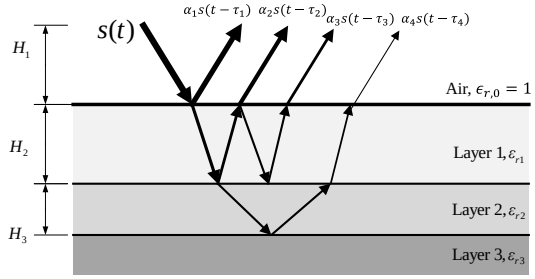

Fig. 3. Pavement configuration.

pattern, the CRB matrix for TDE of GPR echoes is given by [17]

$$\mathrm{CRB}(\boldsymbol{\tau}) = \frac{2}{J}\left\{\left(\frac{\partial \mathbf{r}}{\partial \boldsymbol{\tau}^T}\right)^H \boldsymbol{\Pi}^{\perp}_{\frac{\partial \mathbf{r}}{\partial \boldsymbol{\rho}^T}} \frac{\partial \mathbf{r}}{\partial \boldsymbol{\tau}^T}\right\}^{-1}, \qquad (19)$$

where ∂ is the partial derivative operator; J denotes the number of snapshots; $\boldsymbol{\rho} = \left[\boldsymbol{\tau}^T, \mathbf{p}^T, \sigma_{\mathrm{n}}^2\right]^T$ is unknown parameter vector with time-delay vector $\boldsymbol{\tau} = [\tau_1, \tau_2, \cdots, \tau_K]^T$, source vector $\mathbf{p}{=}s_0\,[\alpha_1, \alpha_2, \cdots, \alpha_K]^T$, and the noise power σ_{n}^2. The projection matrix can be calculated by $\boldsymbol{\Pi}^{\perp}_{\partial \mathbf{r}/\partial \boldsymbol{\rho}^T} = \mathbf{I}_M - \partial \mathbf{r}/\partial \boldsymbol{\rho}^T \left(\left(\partial \mathbf{r}/\partial \boldsymbol{\rho}^T\right)^H \partial \mathbf{r}/\partial \boldsymbol{\rho}^T\right)^{-1} \left(\partial \mathbf{r}/\partial \boldsymbol{\rho}^T\right)^H$.

V. Simulation Results

In the simulations, a three-layer media is tested, as shown in Fig 3. The relative permittivities are $\epsilon_{r1} = 3, \epsilon_{r2} = 8$, and $\epsilon_{r3} = 9$. There are 4 coherent echoes received. The arrival time of the three primary echoes is $\tau_1 = 6.338$ ns, $\tau_2 = 6.667$ ns, and $\tau_4 = 7.423$ ns, respectively. The arrival time of the secondary echo is $\tau_3 = 6.996$ ns. Co-prime sampling with $M_1 = 3$ and $M_2 = 5$ is adopted within frequency band $f \in [1.0, 3.5]$ GHz and frequency interval $\Delta f = 0.1$ GHz. 5001 searching grids are predefined within [5, 10] ns. The SNR is defined as the power ratio between the first echo and the noise. Colored noise is used in the simulations, whose noise pattern is generated as in [3] in each Monte Carlo trail, and is known beforehand.

In the first simulation, the proposed method, MMV-ANM [14], SMV-ANM [12], OMP [10], OGOMP [9] and OGSBI [8] are tested with in a single run with SNR = 10 dB and 100 snapshots. The regulation parameter is $\mu = 0.01$ in the proposed method. Ricker and Gaussian functions are used to simulate the radar pulses in Figs. 4 and 5, respectively. Both MMV-ANM and SMV-ANM fail to estimate τ_3 due to the weak amplitudes and the influence of radar pulse. The

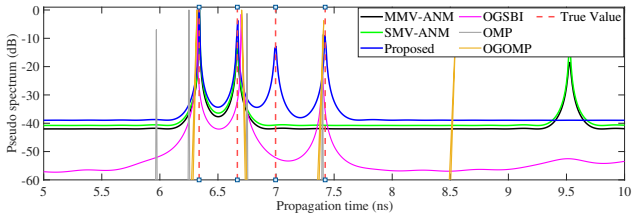

Fig. 4. Pseudo spectra of different algorithms, Ricker wavelet and colored noise are used, SNR = 10 dB, $J = 100$.

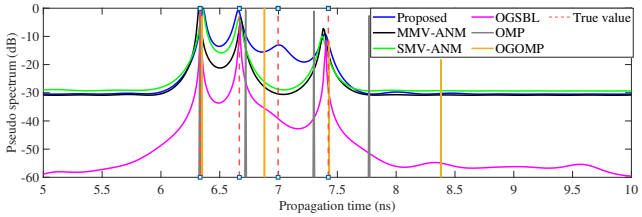

Fig. 5. Pseudo spectra of different algorithms, Gaussian wavelet and colored noise are used, SNR = 10 dB, $J = 100$.

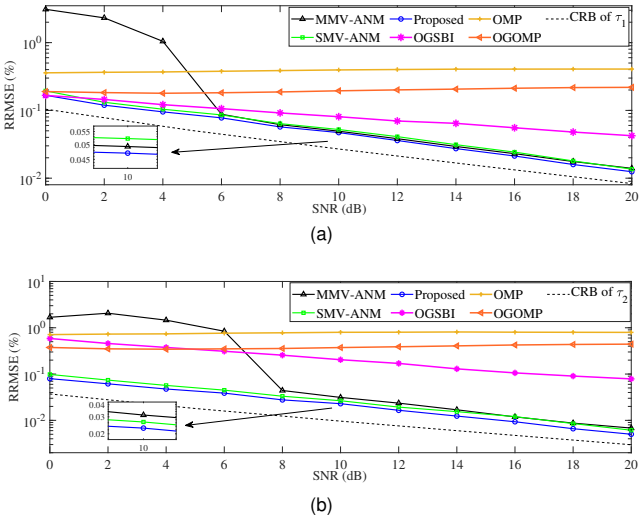

Fig. 6. RRMSE of TDE versus SNR with J = 100. (a) RRMSEs of echo 1, with $\tau_1 = 6.338$ ns. (b) RRMSEs of echo 2, with $\tau_2 = 6.667$ ns.

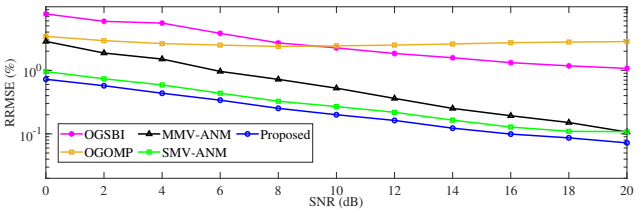

Fig. 7. RRMSE of the estimated thickness $\hat{H}_2$ versus SNR with $J = 100$.

performance of OMP and OGOMP is worse, because of their mismatched data model. Significantly, the proposed method successfully detects the weak echoes and yields the highest estimation accuracy, showing its robustness with different radar pulses and colored noise. In the following simulations, only the first two echoes in presence of Ricker pulse are estimated to make the results comparable.

In the second simulation, the estimation performance of

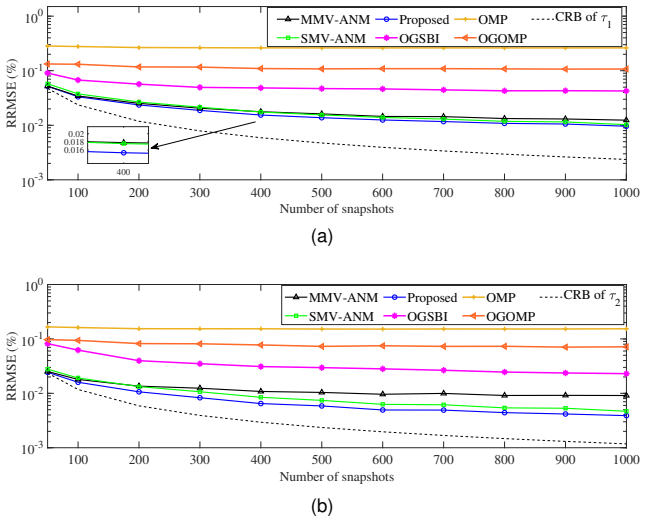

Fig. 8. RRMSE of TDE versus the number of snapshots with SNR = 10 dB. (a) RRMSEs of echo 1, with $\tau_1 = 6.338$ ns. (b) RRMSEs of echo 2, with $\tau_2 = 6.667$ ns.

various methods versus SNR is tested with 500 Monte Carlo trials. Relative root mean square error (RRMSE) [1] serves as the evaluation metric of estimation accuracy. 100 snapshots are observed. Although OMP, OGOMP, and OGSBI realize efficient estimation of the first two echoes, their performance is limited by the basis mismatch, even in the dense dictionary matrix. Therefore, the RRMSEs of these three methods are higher than those of the ANM methods. The performance of the MMV-ANM method is poor at low SNR ($\leq$ 10 dB) because of the influence from the radar pulse. The proposed method outperforms the competitors across all SNR levels. Overall, the proposed approach yields the closest RRMSE to the CRB, yet with lower computational complexity compared with MMV-ANM. The final goal of TDE is to estimate the thickness of layers in GPR detection. In Fig. 7, the thickness estimation performance is evaluated, whose true value is $H_2 = 2.85$ cm. OGSBI and OGOMP perform poorly with higher RRMSEs than the gridless methods. Similarly, the proposed method achieves the lowest RRMSE which highlights its improved performance in thickness estimation.

The third simulation investigates the RRMSEs versus the number of the snapshots with 500 Monte Carlo experiments. The RRMSEs decline with the number of snapshots increasing, indicating an enhanced estimation performance due to the accumulation effect of multi-snapshots. In Fig. 8, the grid-based methods are poorly performing due to the inevitable basis mismatch. On the contrary, the gridless ANM methods have a better performance. Similarly, the proposed method consistently shows the closest performance to the CRB.

Moreover, the average running time of the algorithms is also recorded for 500 runs using a computer with a CPU of 2.4 GHz and 32 GB RAM. By using the 12-point co-prime sampling strategy, the average complexity of the proposed method (0.717 s) is much lower than that of MMV-ANM (1.102 s) and OGSBI (1.273 s).

VI. Conclusions

In this letter, we have developed a co-prime sampling based gridless TDE method for GPR system, taking into account the radar pulse and noise pattern. The enhanced SMV is generated from the generalized eigenspace of data covariance and noise pattern, promoting the detection performance of weak echoes. The complexity of the proposed ANM method is reduced compared with MMV-ANM. Simulations compare the performance of algorithms in presence of Ricker pulse, Gaussian pulse, and colored noise, where the proposed method outperforms its competitors with lower computational complexity and higher accuracy.

References

[1] C. Le Bastard, V. Baltazart, Y. Wang, and J. Saillard, "Thin-pavement thickness estimation using GPR with high-resolution and superresolution methods," *IEEE Transactions on Geoscience and Remote Sensing*, vol. 45, no. 8, pp. 2511–2519, 2007.

[2] M. Sun, J. Pan, C. Le Bastard, Y. Wang, and J. Li, "Advanced signal processing methods for ground-penetrating radar: Applications to civil engineering," *IEEE Signal Processing Magazine*, vol. 36, no. 4, pp. 74–84, 2019.

[3] J. Pan, M. Sun, Y. Wang, C. Le Bastard, and V. Baltazart, "A time-delay estimation approach for coherent GPR signals by taking into account the noise pattern and radar pulse," *Signal Processing*, vol. 176, p. 107654, 2020.

[4] P. Pal and P. P. Vaidyanathan, "Nested arrays: A novel approach to array processing with enhanced degrees of freedom," *IEEE Transactions on Signal Processing*, vol. 58, no. 8, pp. 4167–4181, 2010.

[5] C. Zhou, Z. Shi, Y. Gu, and X. Shen, "DECOM: DOA estimation with combined MUSIC for coprime array," in *2013 International Conference on Wireless Communications and Signal Processing*, 2013, pp. 1–5.

[6] P. Pal and P. P. Vaidyanathan, "Coprime sampling and the MUSIC algorithm," in *2011 Digital Signal Processing and Signal Processing Education Meeting (DSP/SPE)*, 2011, pp. 289–294.

[7] J. Pan, M. Sun, Y. Wang, and X. Zhang, "An Enhanced Spatial Smoothing Technique with ESPRIT Algorithm for Direction of Arrival Estimation in Coherent Scenarios," *IEEE Transactions on Signal Processing*, vol. 68, pp. 3635–3643, 2020.

[8] S. Ji, Y. Xue, and L. Carin, "Bayesian compressive sensing," *IEEE Transactions on signal processing*, vol. 56, no. 6, pp. 2346–2356, 2008.

[9] Z. Tan and A. Nehorai, "Sparse direction of arrival estimation using co-prime arrays with off-grid targets," *IEEE Signal Processing Letters*, vol. 21, no. 1, pp. 26–29, 2014.

[10] J. A. Tropp and A. C. Gilbert, "Signal recovery from random measurements via orthogonal matching pursuit," *IEEE Transactions on Information Theory*, vol. 53, no. 12, pp. 4655–4666, 2007.

[11] Z. Yang, L. Xie, and C. Zhang, "A discretization-free sparse and parametric approach for linear array signal processing," *IEEE Transactions on Signal Processing*, vol. 62, no. 19, pp. 4959–4973, 2014.

[12] Z. Yang, J. Li, P. Stoica, and L. Xie, "Chapter 11 - sparse methods for direction-of-arrival estimation," in *Academic Press Library in Signal Processing, Volume 7*, R. Chellappa and S. Theodoridis, Eds. Academic Press, 2018, pp. 509–581.

[13] C. Zhou, Y. Gu, X. Fan, Z. Shi, G. Mao, and Y. D. Zhang, "Direction-of-arrival estimation for coprime array via virtual array interpolation," *IEEE Transactions on Signal Processing*, vol. 66, no. 22, pp. 5956–5971, 2018.

[14] H. Pan, J. Pan, X. Zhang, and Y. Wang, "Time-delay estimation of ground-penetrating radar using co-prime sampling strategy via atomic norm minimization," *IEEE Transactions on Instrumentation and Measurement*, vol. 73, pp. 1–12, 2024.

[15] S. Lambot, E. Slob, I. van den Bosch, B. Stockbroeckx, and M. Vanclooster, "Modeling of ground-penetrating radar for accurate characterization of subsurface electric properties," *IEEE Transactions on Geoscience and Remote Sensing*, vol. 42, no. 11, pp. 2555–2568, 2004.

[16] E. Warsitz and R. Haeb-Umbach, "Blind acoustic beamforming based on generalized eigenvalue decomposition," *IEEE Transactions on Audio, Speech, and Language Processing*, vol. 15, no. 5, pp. 1529–1539, 2007.

[17] P. Stoica, E. Larsson, and A. Gershman, "The stochastic CRB for array processing: a textbook derivation," *IEEE Signal Processing Letters*, vol. 8, no. 5, pp. 148–150, 2001.